

MICROSTRUCTURE DEVELOPMENT DURING SINTERING OF TiC-Ni₃Al CERMETS

T. N. Tiegs, J. L. Schroeder, F. C. Montgomery, and D. L. Barker

Oak Ridge National Laboratory
Oak Ridge, TN 37831-6087

ABSTRACT

TiC-Ni₃Al cermets are under development for application in diesel engines because of desirable physical properties and wear resistance. Powder compacts with binder contents from 30-50 vol. % were fabricated by pressureless sintering under vacuum followed by low gas pressure isostatic pressing. Increasing the Ni₃Al content improved densification when using prealloyed powders as expected. However, when the Ni₃Al was formed by in-situ reaction synthesis of Ni and NiAl, densification decreased with higher binder contents. The final microstructure consisted of a 'core-rim' structure with TiC cores surrounded by (Ti,W)C rims. In some cases, Ni and Al were also observed in the peripheral region of the rim structure. Grain sizes of the TiC increased with binder content and temperature. Preferred orientation of the Ni₃Al binder phase was observed due to very large grain sizes on the order of millimeters.

INTRODUCTION

Recent research studies have examined cermets based on a matrix consisting of a hard carbide (e.g., TiC or WC) coupled with an intermetallic aluminide alloy (e.g., Ni₃Al or FeAl) binder phase [1-8]. Initial results showed that these composites have exceptional properties and that the binder alloy composition influenced the mechanical properties due to solid solution hardening effects. For instance, fracture toughness values comparable to the very high values obtained in the best commercial cobalt-bonded WC composites can be achieved in the aluminide-bonded carbides. Such extensive toughening is obtained by local plastic deformation in the aluminide phase which means these materials can exhibit very high mechanical reliability (e.g., Weibull modulus > 20 in preliminary studies) [3]. In addition, these cermets can also exhibit high fracture strengths (e.g., in excess of 1 GPa), and these strength levels are retained at temperatures up to 800°C.

Nickel aluminide (Ni₃Al) has several attributes that make it attractive for applications in ceramic-metal composites. Its mechanical behavior is unusual in comparison to other alloys, in that the yield strength increases with increasing temperature up to about 800°C [9,10]. Normally, the intermetallics are brittle in nature, however, it was also discovered that small amounts of boron would make Ni₃Al ductile [10,11]. Thus, its applicability for use as a binder phase for cermets was studied.

The physical properties of these Ni₃Al-based cermets can be tailored by careful selection of matrix and binder, and amounts of each. For instance in the TiC-Ni₃Al system, the thermal expansion coefficients can also be tailored (ranging from ~ 7 to 15 x 10⁻⁶/°C) by modifying the respective volume contents of the different components. The expansion can also be tailored even further by altering the binder phase composition. In addition, the aluminide binder phases provide good oxidation and corrosion resistance [9,11]. The composites are normally non-magnetic, however, with the appropriate substitution of Fe into the Ni₃Al structure (about 20 atom. %), the materials become soft magnetics. Finally, these cermets also exhibit good electrical conductivity allowing them to be machined by electrical discharge machining (EDM) processes; a substantial additional benefit in the manufacture of complex shapes.

While much of the early work involved hot-pressing of the samples to obtain high density materials for mechanical property testing, because of the potential large-scale application, both direct pressureless-sintering of mixtures of carbide and Ni₃Al mixtures and reaction sintering where NiAl + Ni mixtures are substituted for Ni₃Al powders have been investigated [2,4,7]. Other results indicate a melt-infiltration-liquid phase sintering process is also a viable fabrication method [8]. In each process, the equipment requirements and processing conditions are identical to those presently used in the hardmetal industry and thus, they are amenable to cost-effective production.

Because the properties of the aluminide-bonded ceramics are attractive for diesel engine applications, development of these materials was started. Future development of these materials is expected to involve tailoring of the processing to optimize the properties in composite systems with TiC. The issue of most interest was the fabrication of parts using cost-effective processing. Consequently, a study was done to understand the microstructure development during powder processing, sintering and the effect on properties of Ni₃Al-bonded TiC cermets. This present study examined (1) sintering with prealloyed Ni₃Al powder where the alloying additives were incorporated into the powders prior to gas atomization and, (2) reaction sintering with Ni and NiAl powders to form Ni₃Al in-situ. Most of the previous work on Ni₃Al-bonded cermets was done at binder contents of 10-30 vol. %. However, in this study, higher binder contents on the order of 30-50 vol. % were examined because these composites more closely match the thermal expansion of steel.

EXPERIMENTAL PROCEDURE

The powder physical characteristics used in fabrication of the cermets are shown in Table 1. Note the large size of the prealloyed Ni₃Al powder produced by inert gas atomization compared to the other powders. As mentioned, samples were fabricated by two different methods: (1) sintering with prealloyed gas-atomized Ni₃Al powder, or (2) reaction sintering with fine elemental powders to form Ni₃Al in-situ. The compositions studied are given in Table 2. The different processing routes are discussed individually below.

The sintered materials using prealloyed intermetallic powders were fabricated by milling fine TiC powder, with prealloyed Ni₃Al powder. The reaction sintered materials were fabricated by milling appropriate amounts of TiC, Ni, NiAl, and B together to form Ni₃Al in-situ as a reaction product. All of the reaction sintered compositions used a 0.1 wt. % boron addition, which was added as elemental boron. The milling was done in isopropanol for 19 h using WC-Co milling media and 1 wt. % PVP* added as a binder. Media wear during milling contributed ~0.4 wt. % to each of the compositions. For both the sintering using prealloyed intermetallics and the reaction sintering, the mixtures were dried and screened to -100 mesh. Specimens were uniaxially pressed in either 25 or 55 mm diameter steel dies at ~70 MPa (10 ksi) and isopressed at 350 MPa (50 ksi). Sintering was done in a graphite element furnace at temperatures from 1350°C to 1500°C. The heating schedule consisted of a ramp of 10°C/min from room temperature to 1200°C, a 0.5 h hold at 1200°C for degassing, and another ramp at 10°C/min to the final sintering temperature all under vacuum. The temperature was maintained at the sintering temperature for 0.5 h under vacuum followed by an argon gas pressurization to 1 MPa (150 psi) in 10 minutes and a hold under pressure for 10 minutes. The total time at the sintering temperature was 50 minutes.

For all of the test samples, densities were determined by the Archimedes' method. For mechanical property testing, selected samples of high density were machined into bend bar specimens with nominal dimensions of 3 mm x 4 mm x 50 mm. Flexural strength testing was done in four point bending with inner/outer spans of 20 mm/40 mm. Fracture toughness was determined by an indentation and fracture method [12]. Hardness testing was done with a Vickers diamond indenter at a load of 50 kg. Differential thermal analysis (DTA) was done in an argon atmosphere and using a heating rate of 10°C/min. X-ray analysis was performed on powder mixtures both in the as-milled condition and after heating to intermediate temperatures (using the same heating rates as the sintered specimens). X-ray analysis was also performed on machined bulk surfaces of sintered dense composites. Scanning electron microscopy (SEM) was done on polished sections using both secondary electron (SE) and back-scattered electron (BSE) imaging.

* GAF Chemicals, Wayne, NJ: Polyvinylpyrrolidone K-15

Table 1. Physical characteristics of powders.

Powder Type	Supplier/Grade	Ave. Particle Diameter (μm)
TiC	Kennametal (Latrobe, PA)	1.3
Ni	Novamet (Wyckoff, NJ)/ Type 123	5
NiAl	X-Form (Cohoes, NY)	10.9
B	Cerac (Milwaukee, WI)	0.3
Ni ₃ Al	Homogeneous Metals (Clayville, NY)/IC-50 (Ni-11.3 Al-0.6 Zr-0.02 B)	<75 [†]

Table 2. Samples of aluminide-bonded TiC ceramics fabricated by different processing methods to determine the sintering behavior and properties.

Specimen No.	Binder Type	Binder Content (vol. %)	Fabrication Method ^a
DC-10	Ni ₃ Al (IC-50)	30	S/PA
DC-11	Ni ₃ Al (IC-50)	40	S/PA
DC-12	Ni ₃ Al (IC-50)	50	S/PA
DC-13	Ni ₃ Al	30	RS/E
DC-14	Ni ₃ Al	40	RS/E
DC-15	Ni ₃ Al	50	RS/E

^a

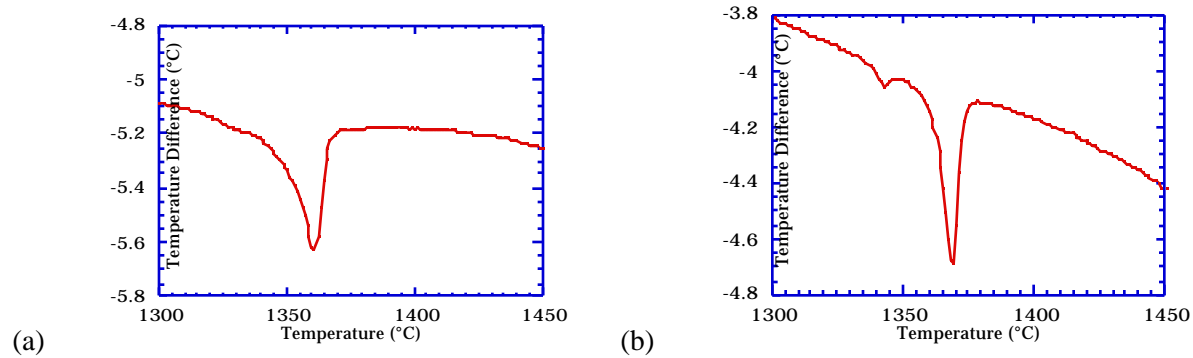


Fig. 1. DTA results on (a) prealloyed Ni₃Al-TiC (DC-11); and (b) Ni/NiAl-TiC (DC-14) mixtures.

The densification results are summarized in Fig. 4. As indicated, high densities were obtained for most compositions at temperatures of 1400°C, where a liquid phase is present. At temperatures of 1350°C, with little to no liquid phase present, all of the densification was associated with solid state diffusion processes. Even in that case, significant densification takes place. As expected, lower densities were observed with the 30% content of the Ni₃Al liquid phase in comparison to the higher volume contents. Much of the reason for the low densities is attributable to remnant large pores as shown in Fig. 5. These large pores are most likely due to the formation of a semi-rigid TiC network that forms after the liquid is wicked into the surrounding TiC powders by capillary action. Because of the large size of the pore it is difficult to eliminate and prevents shrinkage during sintering. At the higher volume contents of Ni₃Al, the occurrence of these pores was less. At higher binder contents, particle rearrangement is dominant, no TiC networks are formed and there is sufficient liquid present to fill the voids. In any case, their appearance could probably be eliminated by using a sinter-HIP cycle at higher gas pressures than used in the present study, such as those used for WC-Co hardmetals.

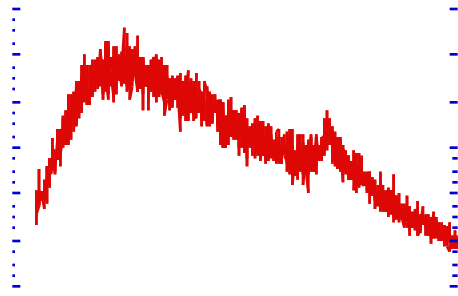
X-ray analysis on the bulk surfaces of the sintered materials showed the presence of only TiC and Ni₃Al (Figs. 6 and 7). The TiC peaks for the materials sintered at 1400°C showed some minor peak broadening which is most likely indicative of the formation of the solid solution with W and development of the rim structure. At 1500°C, the TiC peaks were better defined, however, the peaks were shifted slightly also indicating the formation of a solid solution.

While the TiC peaks were easily discernible in all the x-ray patterns, the Ni₃Al peaks were quite variable in both width and intensity from sample to sample. The main reason for the broad Ni₃Al peak widths is believed due to the considerable solid solution that can occur in these composite systems. Quantitative EDX of the binder phase for a TiC-50 vol. % Ni₃Al sample fabricated by sintering with prealloyed Ni₃Al at 1500°C (DC-12) showed the following content (atomic %): Ni - 72.40; Al - 24.77; and Ti - 2.83. This corresponds to a composition of Ni_{2.9}Al_{0.99}Ti_{0.11} and indicates the binder composition is altered by solution of the TiC into the liquid phase during sintering. Titanium is supposed to predominantly occupy aluminum sites when it is incorporated into the Ni₃Al structure [9]. However, based on the apparent stoichiometry of the binder, most of the substitution seems to be associated with the Ni sites. Such wide ranging substitutions would account for the broad x-ray peaks observed in the sintered specimens. It should also be noted that because of the large difference in thermal expansions between the component phases, the Ni₃Al binder is under tension. Such stresses could also contribute to shifts in the observed x-ray patterns.

In general, the strongest Ni₃Al x-ray peaks, as expected, were associated with the samples with the high binder contents. However, in some cases, the Ni₃Al was barely detectable even though appreciable amounts were known to be present (Figs. 6a, 6c, 7a, and 7b). The only plausible explanation for such observations was that the Ni₃Al had some preferred orientation in the specimens that could be affecting the reflection intensities. X-ray patterns from the same specimen (DC-15) were taken both parallel and perpendicular to the thickness direction (Fig. 8). As shown, a significant difference in the Ni₃Al peak intensities is apparent. To estimate the degree of preferred orientation, rocking scans, where the specimen is rotated about the focal plane axis, were performed at the Ni₃Al peak of $2\theta = 43.5^\circ$. A rocking scan that

shows no change in intensity with angle indicates no preferred orientation. However, preferred orientation is evident when variable intensities are observed. The results, shown in Fig. 9 indicate the existence of some preferred orientation of the Ni_3Al . The rocking scans parallel to the thickness (Figs. 9a and 9c) both exhibit varying x-ray intensity signifying orientation is present. In the case of the rocking scans perpendicular to the thickness, the results were mixed. The specimen sintered at 1400°C (DC-15-2, Fig. 9b) reveals no apparent orientation effects, although the low count rate over the entire scan may have contributed to the effect. However, for the specimen sintered at 1500°C (DC-15-4, Fig. 9d), the variable x-ray intensity implies orientation of the Ni_3Al perpendicular to the thickness.

Orientation effects can be caused by several morphologies, but the most common is the occurrence of



(a)

size can be attributable to only a few possible differences: (1) solubility of the TiC; (2) diffusion in the liquid phase; or (3) kinetics of solution and reprecipitation at the TiC interface. The only significant difference between the Ni₃Al in the prealloyed versus the reaction sintered materials is the 0.6 wt. % Zr in the prealloyed powder. This small amount of Zr should have only a minor effect on the solubility of TiC and diffusion in the liquid phase. However, the Zr would act as a powerful oxygen getter in the system due to the high free energy of formation and stability of ZrO₂. This oxygen gettering could significantly influence the wetting between the TiC and the liquid phase and thus affect the solution-reprecipitation kinetics. Small amounts of surface oxygen are well known to adversely affect the wetting between carbides and molten metals and in a similar fashion, minor additions of Mo to Ni have been shown to reduce the contact angle with TiC from 17° to 0° [20-22].

A summary of the flexural strength results is shown in Fig. 13. As indicated, the strength generally increased with increasing Ni₃Al content. This is most likely due to the slight improvement in densification with the higher binder contents. The results also show a significant difference between the composites made with prealloyed powders and those made by reaction sintering of elemental powders. The reason for the poor strengths of the reaction sintered materials is being determined. Previous results on TiC-40 vol. % Ni₃Al composites fabricated by reaction sintering showed strengths of approximately 1150 MPa, which is more similar to those on the materials made with prealloyed powders in the present results [4].

Like the strength, the fracture toughness generally increased with increasing Ni₃Al volume content as shown in Fig. 14. That was anticipated. Also like the strength results, the composites made with prealloyed powders exhibited higher toughness than those fabricated by reaction sintering. In all cases, the fracture toughness was $K_{Ic} > 10 \text{ MPa} \cdot \text{m}$ and for the composite with 50 vol. % Ni₃Al and fabricated with prealloyed Ni₃Al powders was $> 25 \text{ MPa} \cdot \text{m}$. These values are exceptional and were the basis for the choice of these types of composites for development for diesel engine applications. The high toughness values are a result of the plastic deformation and crack bridging effects of the Ni₃Al binder. These effects are illustrated in Figs. 15 and 16 which show crack behavior at the tips of the indents introduced during hardness and toughness testing. Crack bridging is readily evident in Fig. 15. Brittle fracture of the TiC is observed even in isolated grains away from any cracks in the binder. The indent hardness was measured on several specimens sintered at different temperatures and is summarized in Fig. 17. As shown, the hardness decreased with increasing Ni₃Al content and TiC grain size with the samples fabricated with prealloyed powders having slightly higher values.

CONCLUSIONS

As-received Ni₃Al and NiAl powders are crystalline in nature and during ball milling with TiC, to form the composite mixtures, become highly disordered due to extensive deformation. Upon heating, the Ni₃Al and NiAl undergo recrystallization. At higher temperatures between 1200°C and 1300°C, the Ni/NiAl mixtures react with one another in the solid state to form Ni₃Al in-situ. Liquid formation, for both the prealloyed powders and the reaction sintered materials, takes place at temperatures around 1360°C to 1370°C.

Liquid phase sintering of the composites with 30 to 50 vol. % Ni₃Al results in high densities being achieved for sintering temperatures 1400°C. The final microstructures consist of TiC grains and a surrounding matrix of a (Ni,Ti)₃Al. The TiC grains are made up of a core region of pure TiC and a rim region of a (Ti,W)C solid solution. The W was a contaminant from milling media wear during powder processing. In some cases Ni and Al were also observed in the peripheral areas of the rim structure and are believed to be incorporated during reprecipitation when cooling from the sintering temperature. The Ni₃Al precipitates as large grains on the order of a millimeter in size, which enable them to encompass multitudes of TiC grains.

ACKNOWLEDGMENTS

Research sponsored by both the Propulsion System Materials Program, DOE Office of Transportation Technologies, and the Advanced Industrial Materials Program, DOE Office of Industrial Technologies, under contract DE-AC0596OR22464 with Lockheed Martin Energy Research Corp.

REFERENCES

1. T. N. Tieg, K. B. Alexander, K. P. Plucknett, P. A. Menchhofer, P. F. Becher and S. B. Waters, "Ceramic Composites With a Ductile Ni₃Al Binder Phase," *Mater. Sci. Eng.*, Vol. A209, No. 1-2, 243-47 (1996).
2. T. N. Tieg, P. A. Menchhofer, K. P. Plucknett, K. B. Alexander, and P. F. Becher, "Hardmetals Based on Ni₃Al as the Binder Phase" pp. 211-218 in *Internat. Conf. on Powd. Metall., Met. Powd. Indus. Fed.*, Princeton, NJ (1995).
3. K. P. Plucknett, T. N. Tieg, P. A. Menchhofer, P. F. Becher and S. B. Waters, "Ductile Intermetallic Toughened Carbide Matrix Composites," *Ceram. Eng. Sci. Proc.*, 17[3]314-321 (1996).
4. T. N. Tieg, K. P. Plucknett, P. A. Menchhofer and P. F. Becher, "Development of Ni₃Al-Bonded WC and TiC Cermets", pp. 339-357 in *Internat. Symp. Nickel and Iron Aluminides*, ASM International, Metals Park, OH (1997).
5. J. H. Schneibel, R. Subramanian, K. B. Alexander, and P. F. Becher, "Processing and Properties of FeAl-Bonded Composites," pp. 329-338 in *Internat. Symp. Nickel and Iron Aluminides*, ASM International, Metals Park, OH (1997).
6. R. Subramanian and J. H. Schneibel, "Processing Iron-Aluminide Composites Containing Carbides or Borides," *J. Metals*, 49[8] 50-54 (1997).
7. T. N. Tieg, P. A. Menchhofer, K. P. Plucknett, P. F. Becher, C. B. Thomas and P. K. Liaw, "Comparison of Sintering Behavior and Properties of Aluminide-Bonded Ceramics." *Ceram. Eng. Sci. Proc.*, 19[3] 447-455 (1999).
8. K. P. Plucknett, P. F. Becher, and R. Subramanian, "Melt-Infiltration Processing of TiC/Ni₃Al Composites," *J. Mater. Res.*, 12 [10] 2515-2517 (1997).
9. C. T. Liu and J. O. Stiegler, "Ordered Intermetallics," *ASM Handbook*, Vol. 2, pp. 913-942, ASM International, Metals Park, OH (1990).
10. S. M. Copley and B. H. Kear, *Trans. Metall. Soc. AIME*, Vol. 239, 977-985 (1967).
11. C. T. Liu and V. K. Sikka, "Nickel Aluminides for Structural Use," *J. Metals*, 38[5]19-21(1986).
12. P. Chantikul, G. R. Anstis, B. R. Lawn and D. B. Marshall, "A Critical Evaluation of Indentation Techniques for Measuring Fracture Toughness: II, Strength Method," *J. Am. Ceram. Soc.*, **64** [9] 539-543 (1981).
13. *Phase Equilibrium Diagrams*, Vol. 10, A. E. McHale (ed.), Fig. 9017, pp. 345, Am. Ceram. Soc., Westerville, OH (1994).
14. P. Ettmayer, "Hardmetals and Cermets," *Annual Rev. Mater. Sci.*, Vol. 19, 145-164 (1989).
15. A. Doi, T. Nishikawa, and A. Hara, pp. 329-340 in *Science of Hard Materials*, R. K. Viswanadham, D. J. Rowcliffe, and J. Gurland (eds.), Plenum Press, New York (1983).
16. M. H. Lewis, "Crystallization of Grain Boundary Phases in Silicon Nitride and Sialon Ceramics," pp. 217-231 in *Tailoring of Mechanical Properties of Si₃N₄ Ceramics*, M. Hoffmann and G. Petzow (eds.), Kluwer Academic Pub., Boston, MA (1994).
17. J. K. Yang and H.-C. Lee, "Microstructure Evolution During the Sintering of a Ti(C,N)-Mo₂C-Ni," *Mater. Sci. Eng.*, Vol. A209, No. 1-2, 213-217, (1996).
18. H. Yoshimura, T. Sugizawa, K. Nishigaki, and H. Doi, *Int. J. Refractory Metals and Hard Metals*, 33 [4] 170-174 (1983).
19. R. Warren, *J. Mater. Sci.*, Vol. 3, 471-485 (1968).
20. L. S. Williams and P. Murray, "Bonding in Cermets." *Metallurgia*, 49, 210-217 (1954).
21. M. Humenik and N. M. Parikh, "Cermets and Physical Properties of Cermet Systems," *J. Am. Ceram. Soc.*, 39, 61-62 (1956).
22. M. Humenik and T. J. Whalen, "Physiochemical Aspects of Cermets," pp. 6-49 in *Cermets*, Reinhold, New York (1960).

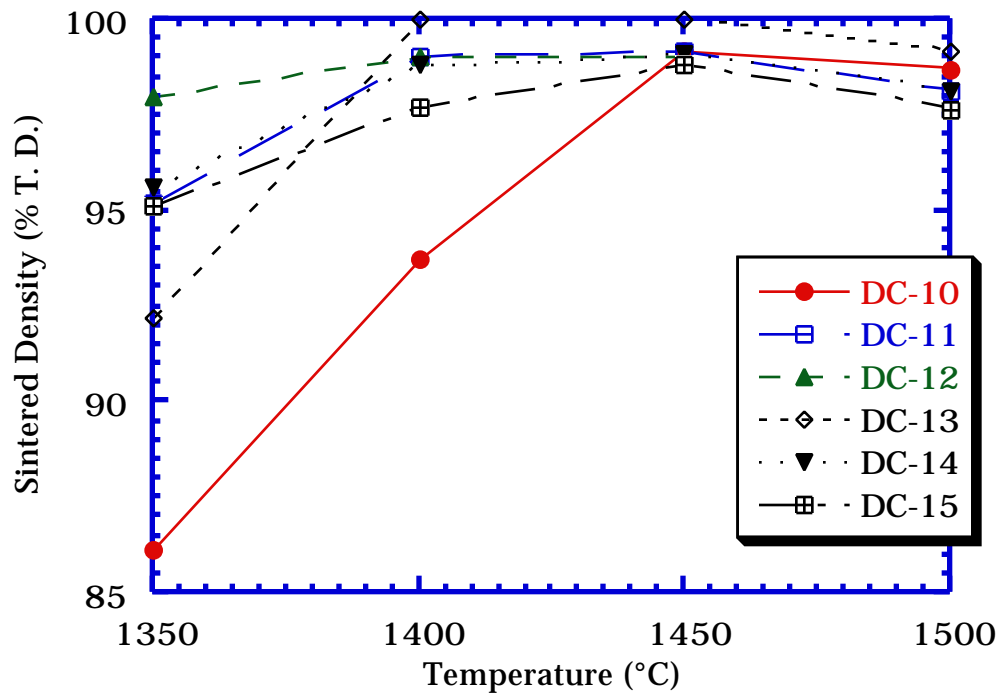


Fig. 4. Summary of densification behavior of Ni₃Al-bonded TiC composites.

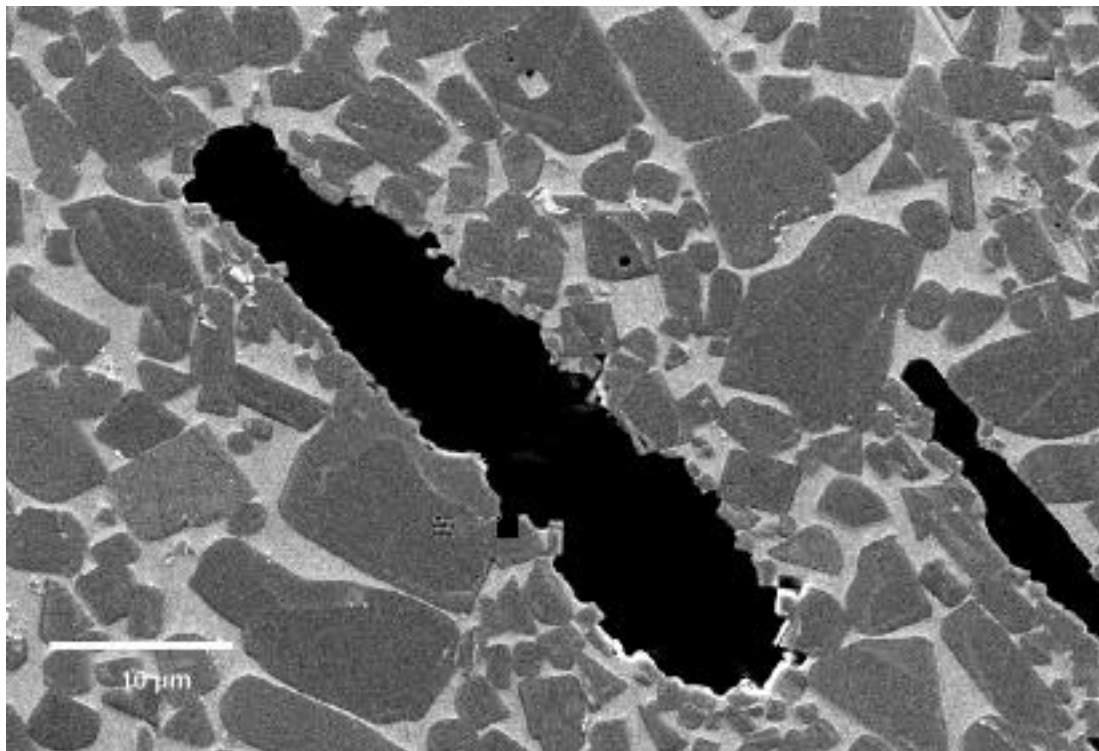


Fig. 5. SE image of microstructure of TiC-30 vol. % Ni₃Al fabricated by sintering with prealloyed Ni₃Al (DC-10) at 1400°C. Large pore was remnant from large prealloyed Ni₃Al powders.

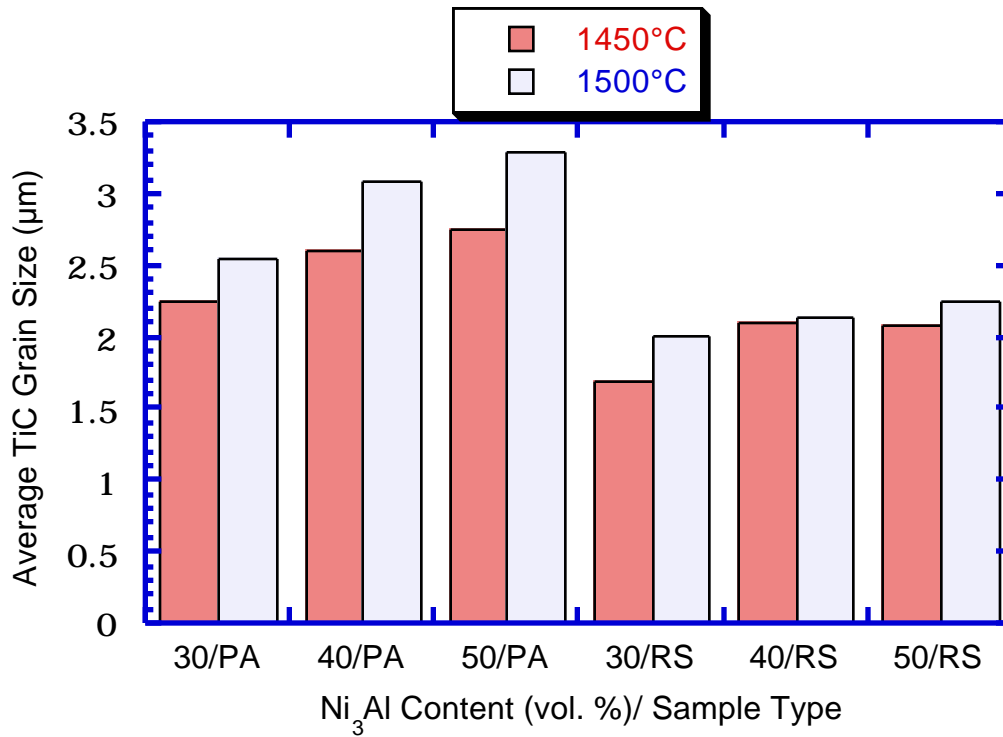


Fig. 12. Summary of average TiC grain size on Ni₃Al-bonded TiC composites fabricated using either prealloyed Ni₃Al powders (PA) or reaction sintered with elemental powders (RS). Sintering was done at the specified temperature.

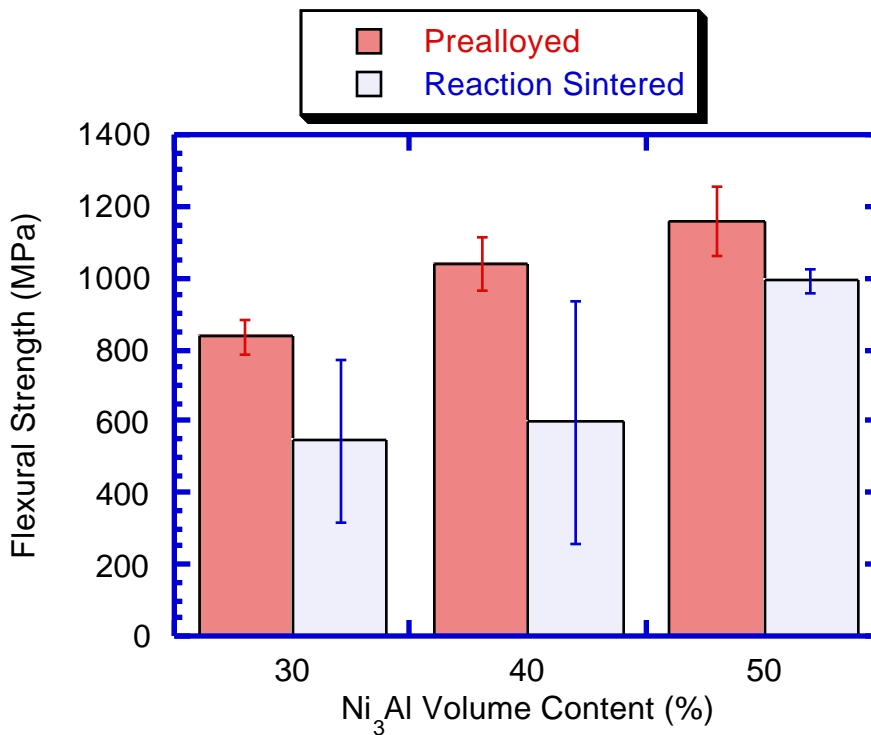


Fig. 13. Summary of flexural strength results on Ni₃Al-bonded TiC composites fabricated using either prealloyed Ni₃Al powders or reaction sintered with elemental powders. Sintering was done at 1450°C.

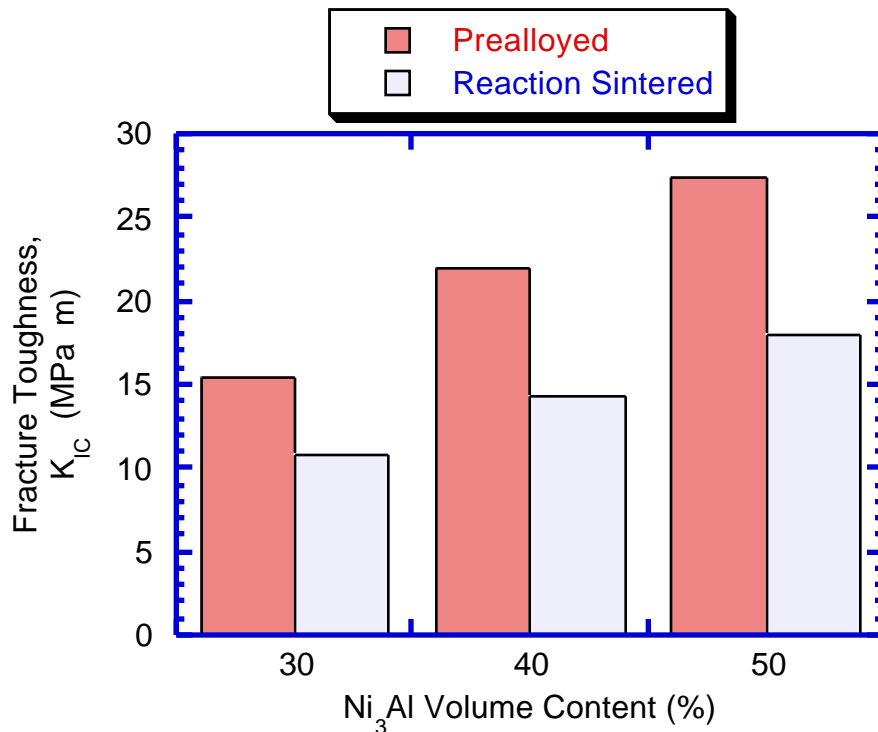


Fig. 14. Summary of fracture toughness results on Ni₃Al-bonded TiC composites fabricated using either prealloyed Ni₃Al powders or reaction sintered with elemental powders. Sintering was done at 1450°C.

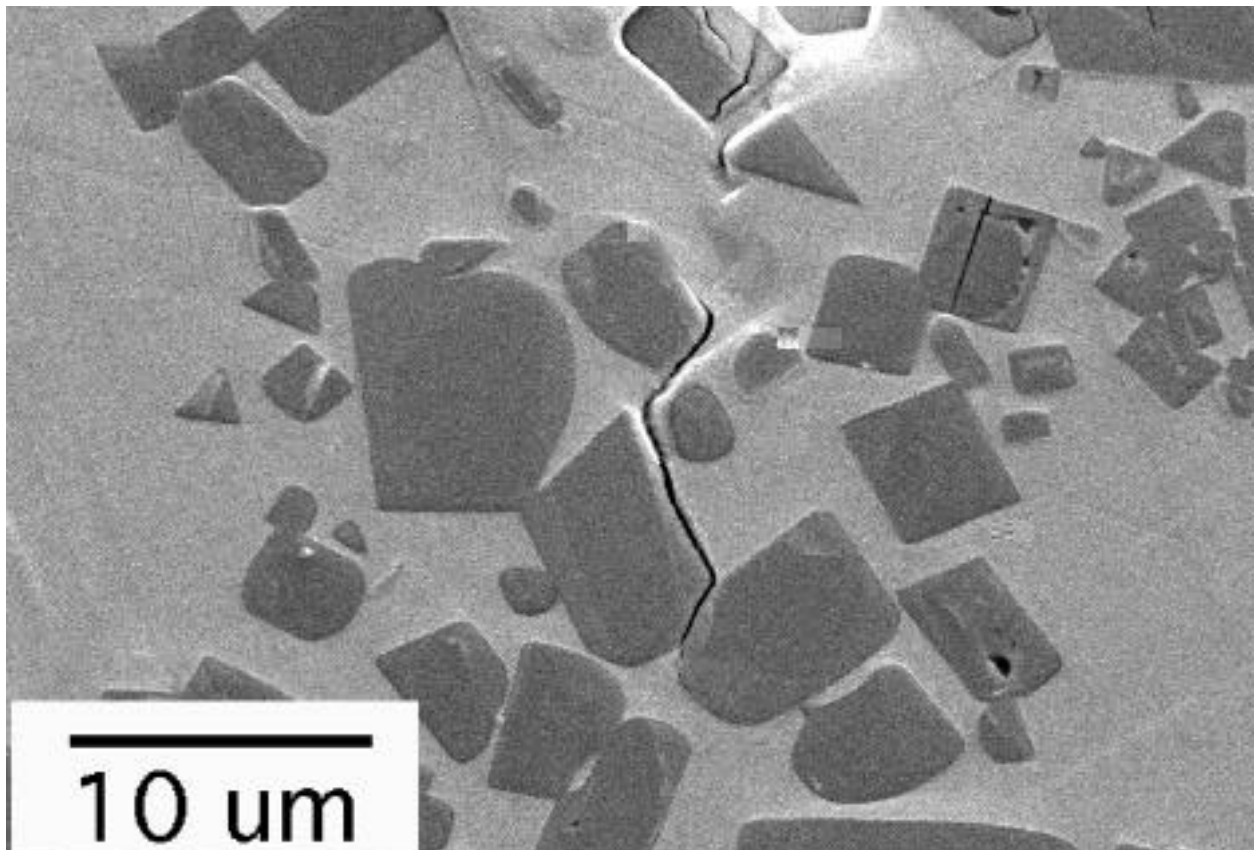
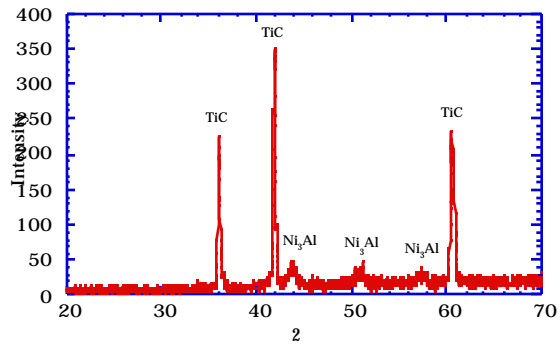
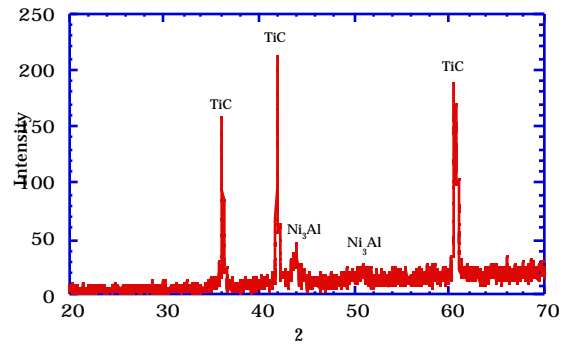


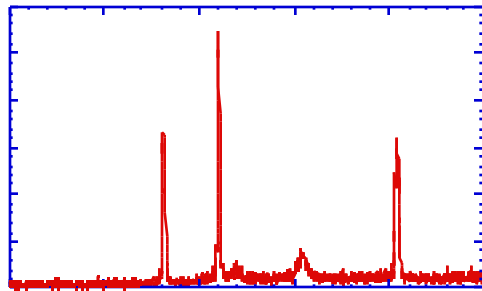
Fig. 15. SE image of microstructure of TiC-50 vol. % Ni₃Al fabricated by sintering with prealloyed Ni₃Al (DC-12) at 1500°C. Crack bridging by the binder is evident at indent tip (top of photograph).



(b)



(c)



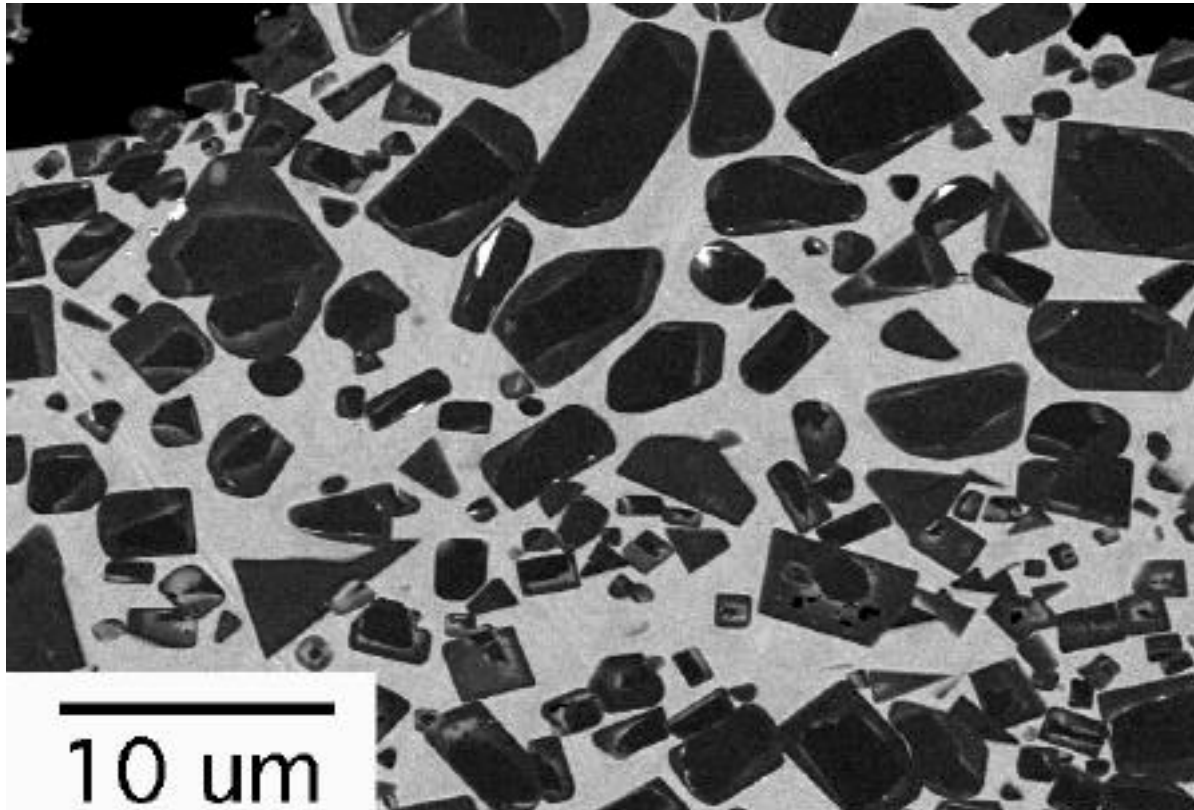


Fig. 10. BSE image of microstructure of TiC-40 vol. % Ni₃Al fabricated by sintering with prealloyed Ni₃Al (DC-11) at 1450°C. TiC particles exhibit a 'core-and-rim' morphology.

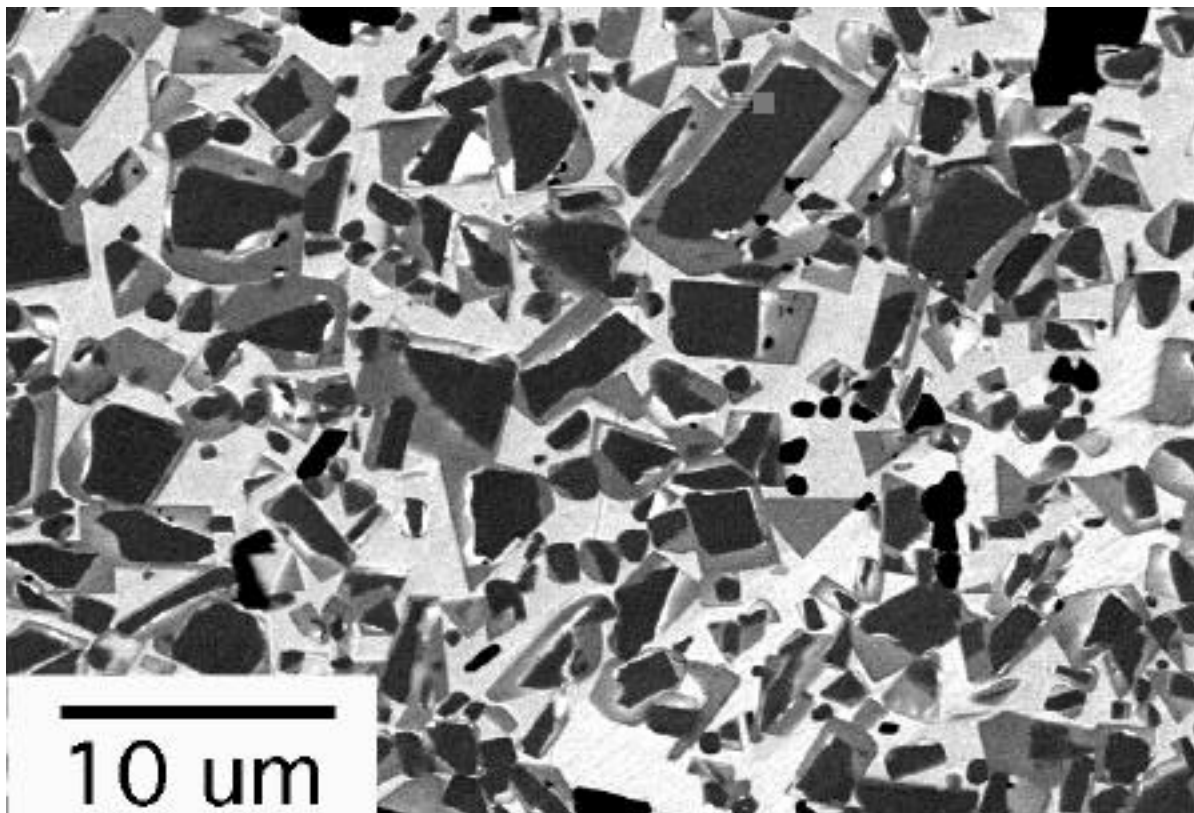


Fig. 11. BSE image of microstructure of TiC-40 vol. % Ni₃Al fabricated by reaction sintering with Ni/NiAl mixtures (DC-14) at 1450°C. TiC particles exhibit a 'core-and-rim' morphology.

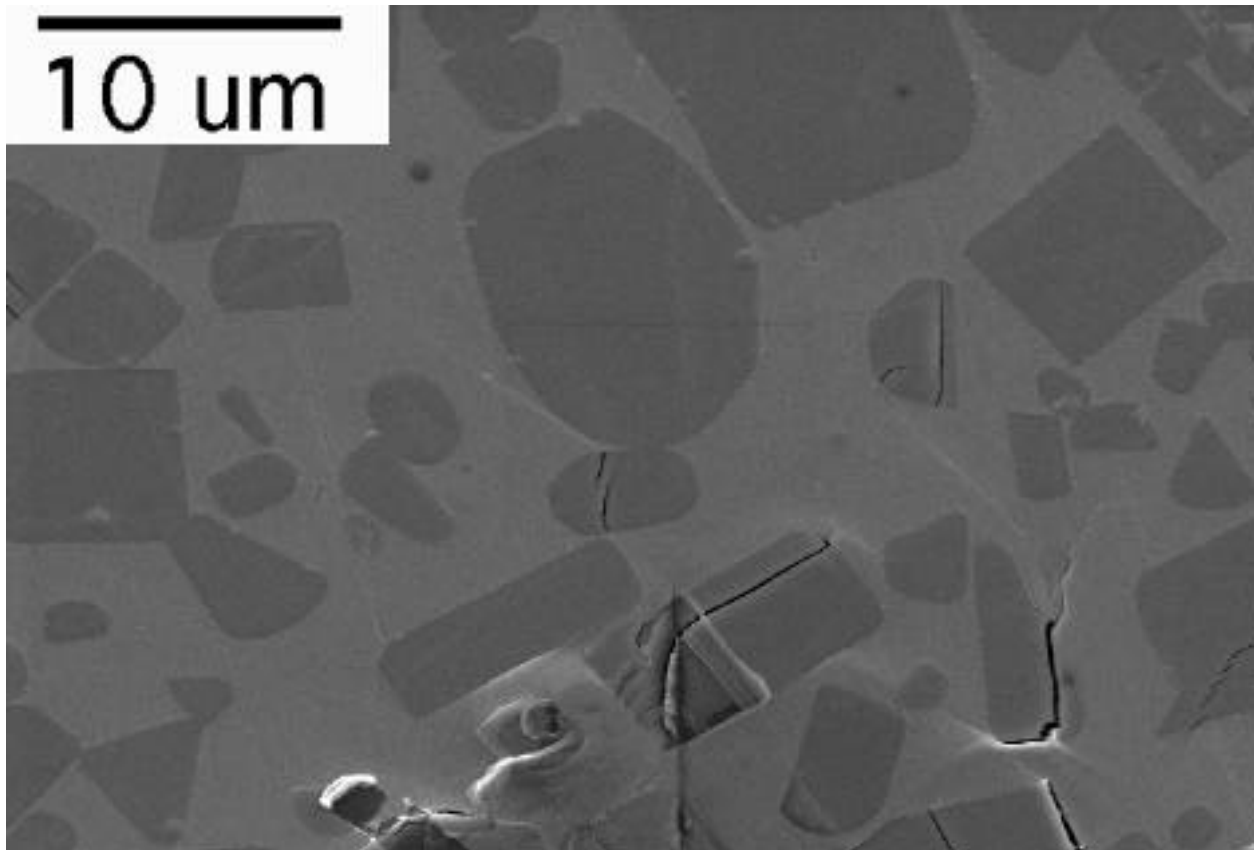


Fig. 16. SE image of microstructure of TiC-50 vol. % Ni₃Al fabricated by reaction sintering with Ni/NiAl mixtures (DC-15) at 1500°C. Cracking of the TiC is evident around indent tip (bottom of photograph).

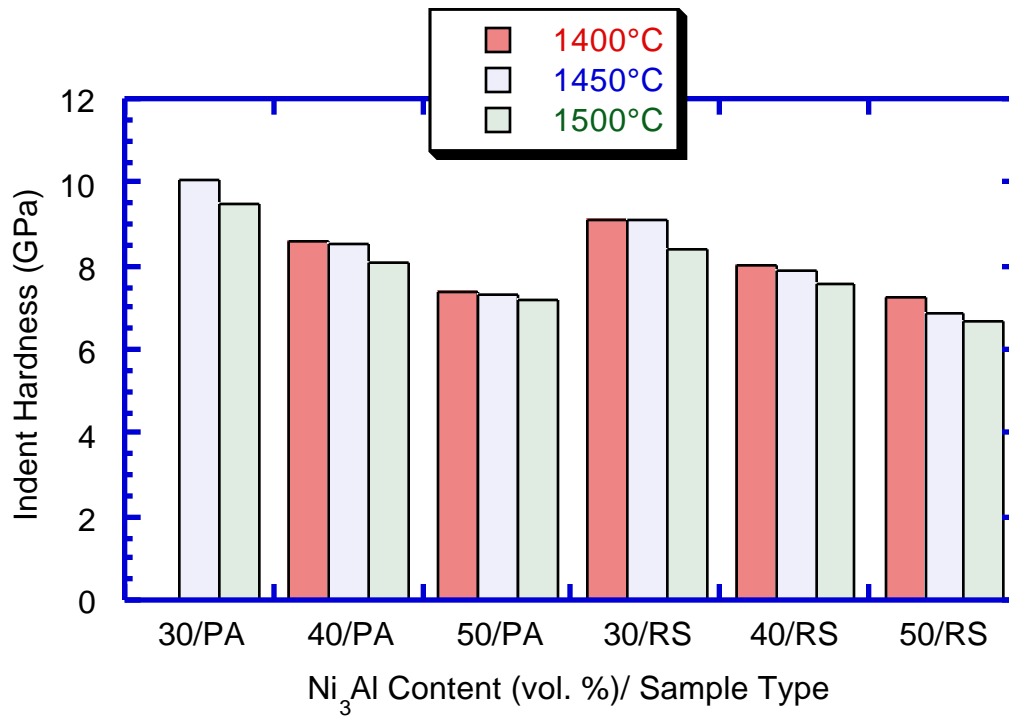
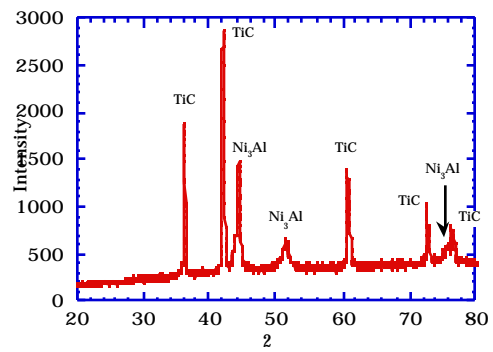
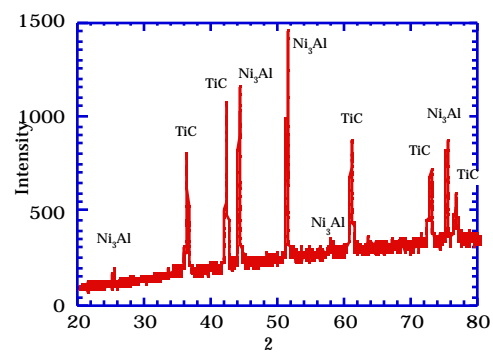


Fig. 17. Summary of indent hardness results on Ni₃



(a)



(b)

